Recent updates from JAM

Nobuo Sato

INT workshop,
Jun 10 2024

Jefferson Lab

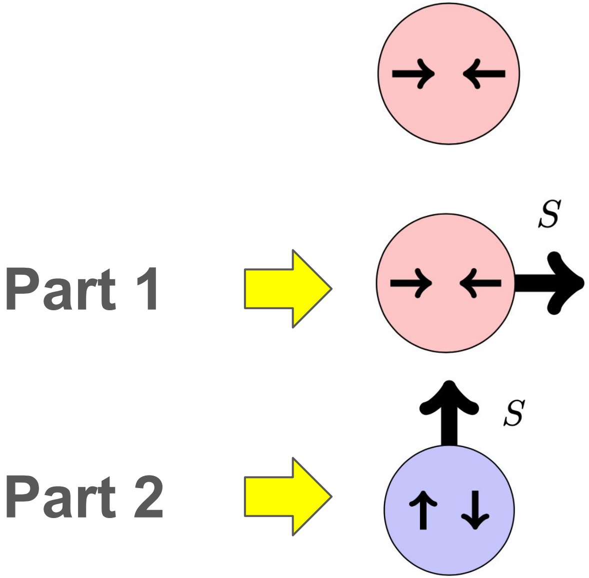

$$f = f_{\rightarrow} + f_{\leftarrow}$$

$$\Delta f = f_{\rightarrow} - f_{\leftarrow}$$

Helicity distribution

$$\delta_{\mathrm{T}} f = f_{\uparrow} - f_{\downarrow}$$

Transversity

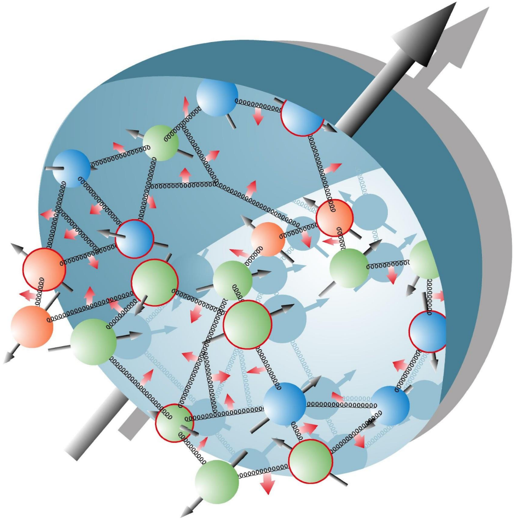

Updates on gluon helicity PDF

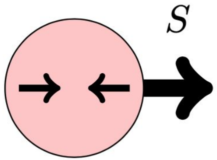

$$\Delta f = f_{\rightarrow} - f_{\leftarrow}$$

Helicity distribution

Zhou, NS, Melnitchouk ‘22
Karpie, Whitehill, Melnitchouk, Monahan, Orginos, Qiu, Richards, NS, Zafeiropoulos ‘23
Hunt-Smith, Cocuzza, Melnitchouk, NS, Thomas, White ‘24

How well do we know the gluon polarization in the proton?

Y. Zhou, N. Sato, and W. Melnitchouk (Jefferson Lab Angular Momentum (JAM) Collaboration)
Phys. Rev. D **105**, 074022 – Published 25 April 2022

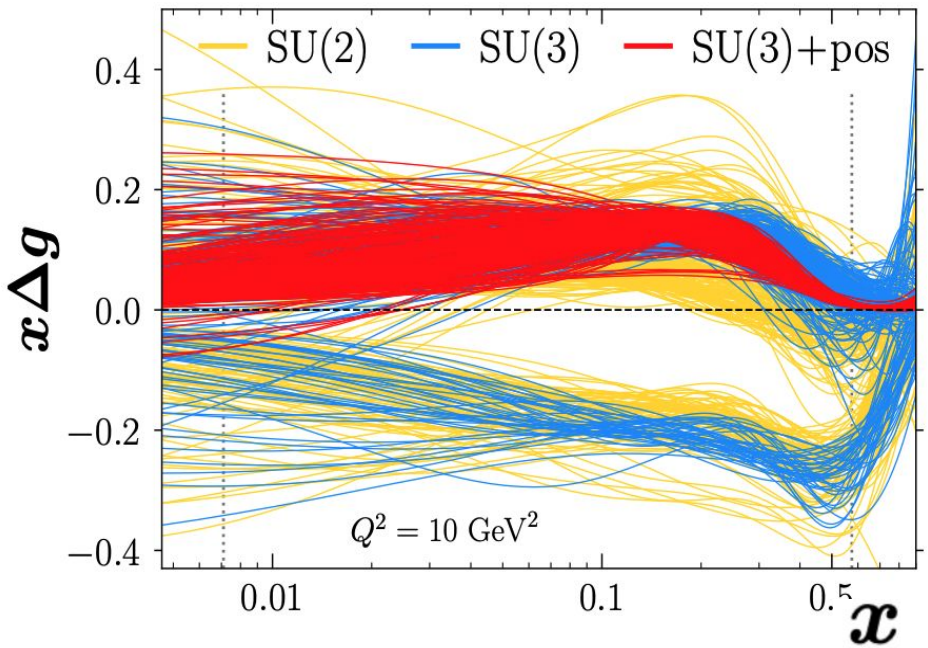

- Sign of gluon-hpdf is not uniquely determined by existing experimental data (DIS W^2 > 10 GeV^2)
- PDF positivity constraints + data strongly disfavors negative g-hpdf
- Negative g-hpdf violates significantly pdf positivity constraint
- PDF positivity is not a strict requirement in QCD

$$|\Delta g| < g$$

PDF positivity constraint

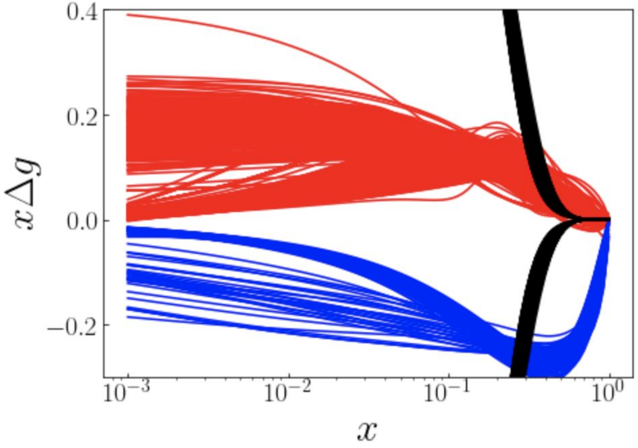

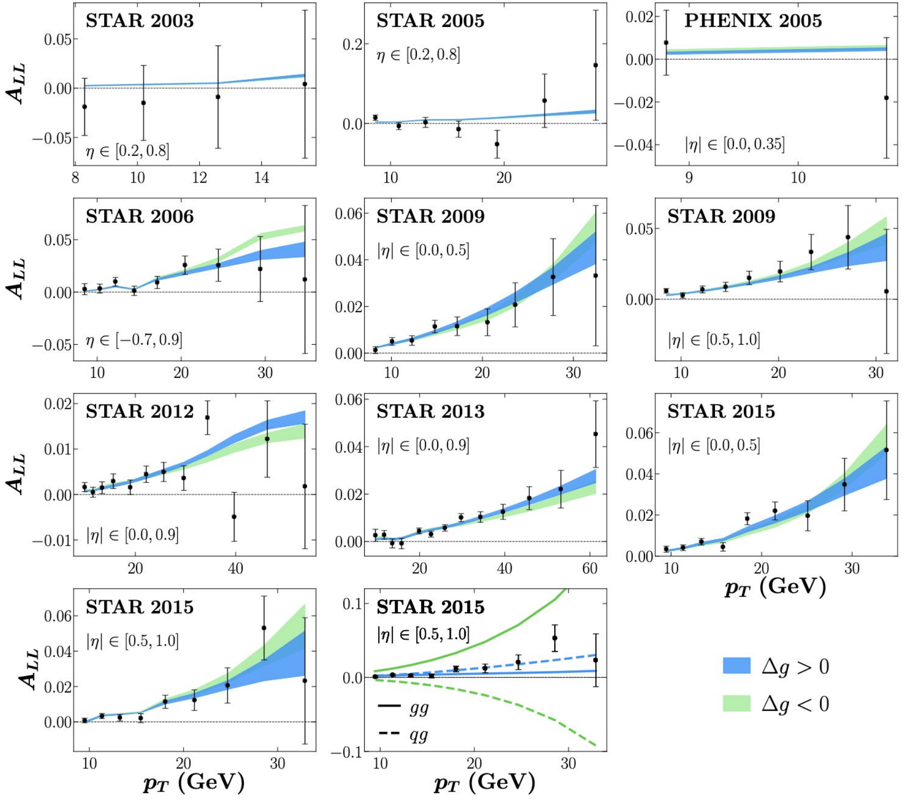

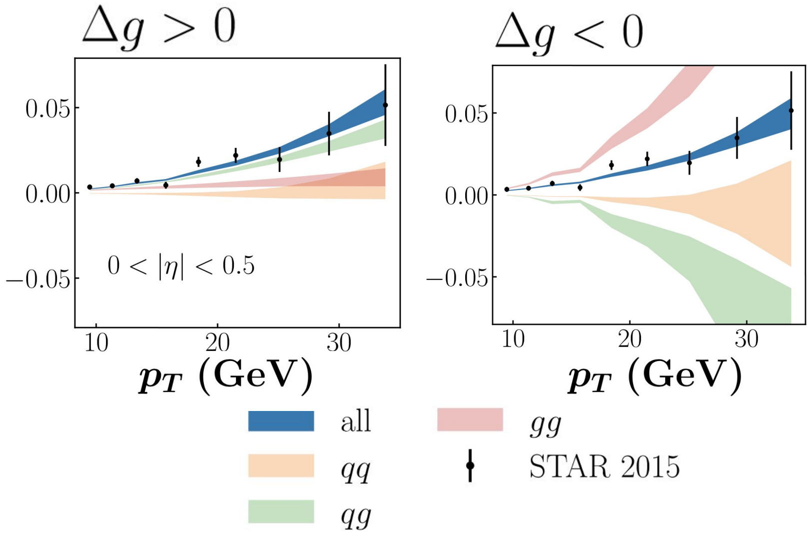

$$A_{LL}^{\text{jet}}(p_T, y) \propto a_{gg}[\Delta g \otimes \Delta g] + \sum_q a_{qg}[\Delta q \otimes \Delta g] + \sum_{q,q'} a_{qq'}[\Delta q \otimes \Delta q'] + \mathcal{O}(\alpha_s),$$

$$|A_{LL}| < 1$$

g-hpdf enters quadratically, and different subchannels contribute with different signs and strengths

Measurement of charged pion double spin asymmetries at midrapidity in longitudinally polarized $p + p$ collisions at $\sqrt{s}$ = 510 GeV

PHENIX Collaboration • U.A. Acharya (Georgia State U.) et al. (Apr 6, 2020)

Published in: *Phys.Rev.D* 102 (2020) 3, 032001 • e-Print: 2004.02681 [hep-ex]

Charged-pion cross sections and double-helicity asymmetries in polarized p+p collisions at $\sqrt{s}$=200 GeV

PHENIX Collaboration • A. Adare (Colorado U.) et al. (Sep 5, 2014)

Published in: *Phys.Rev.D* 91 (2015) 3, 032001 • e-Print: 1409.1907 [hep-ex]

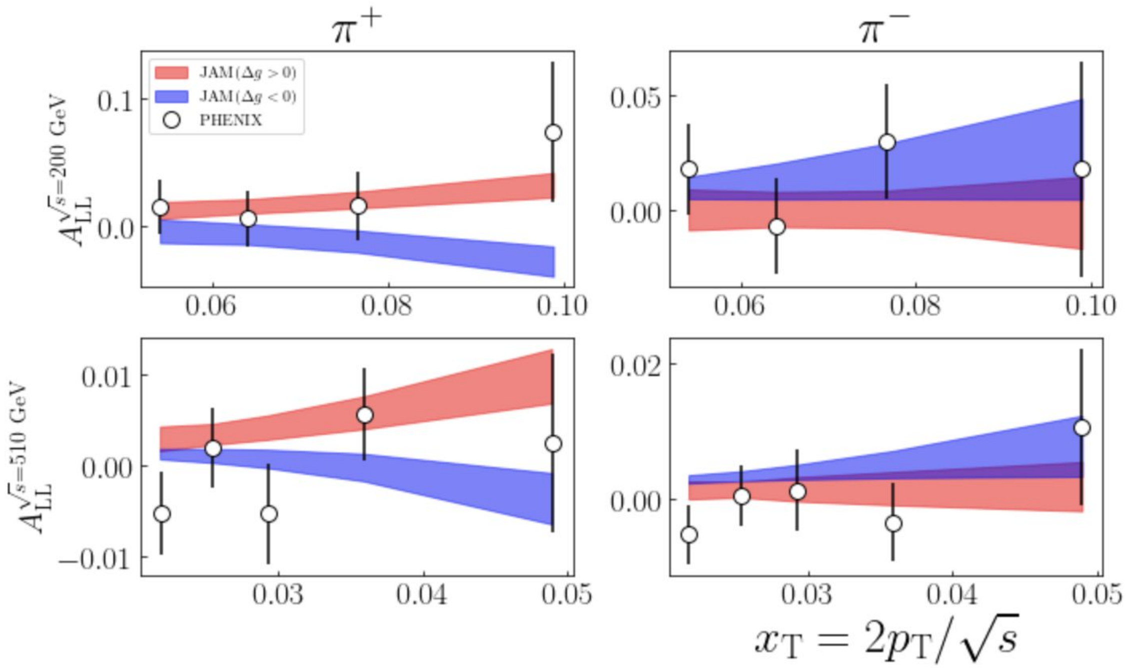

- PHENIX collaboration stated that the gluon spin contribution is positive
- The two solutions for g-hpdf found by JAM describe the data equally well

Measurement of Direct-Photon Cross Section and Double-Helicity Asymmetry at $\sqrt{s} = 510$ GeV in $\vec{p} + \vec{p}$ Collisions

PHENIX Collaboration • U. Acharya (Georgia State U., Atlanta) et al. (Feb 16, 2022)

e-Print: 2202.08158 [hep-ex]

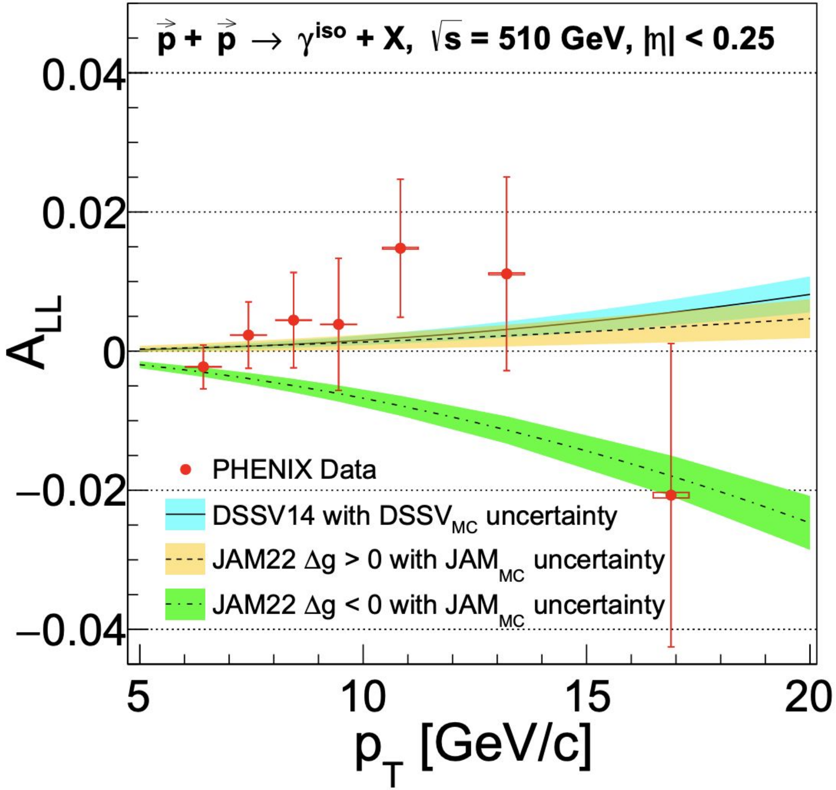

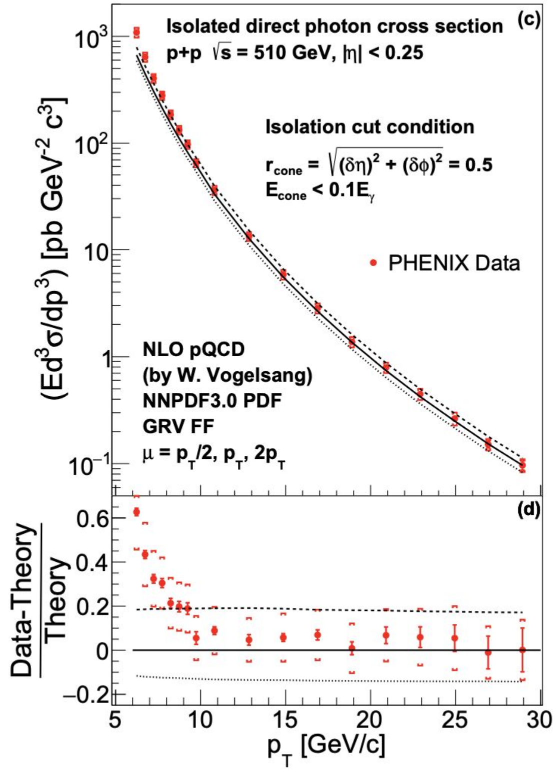

- PHENIX collaboration stated that negative g-hpdf is disfavored by more than 2.8 σ

- However, only last 3 high-pT A_LL points are well described in pQCD (see denominator of A_LL)

Gluon helicity from global analysis of experimental data and lattice QCD Ioffe time distributions

J. Karpie, R. M. Whitehill, W. Melnitchouk, C. Monahan, K. Orginos, J.-W. Qiu, D. G. Richards, N. Sato, and S. Zafeiropoulos (Jefferson Lab Angular Momentum and HadStruc Collaborations)

Phys. Rev. D **109**, 036031 – Published 27 February 2024

Toward the determination of the gluon helicity distribution in the nucleon from lattice quantum chromodynamics

HadStruc Collaboration • Colin Egerer (Jefferson Lab) et al. (Jul 18, 2022)

Published in: *Phys.Rev.D* 106 (2022) 9, 094511 • e-Print: 2207.08733 [hep-lat]

$$\widetilde{M}^{\mu\nu;\alpha\beta}(p,z) = \langle p|F^{\mu\nu}(0)W(0;z)\widetilde{F}^{\alpha\beta}(z)|p\rangle$$

$$\widetilde{\mathfrak{M}}(\nu,z^2) = \frac{\widetilde{M}_{00}(p,z)/p_0p_3Z_L(z_3/a)}{M_{00}(p=0,z)/m^2}$$

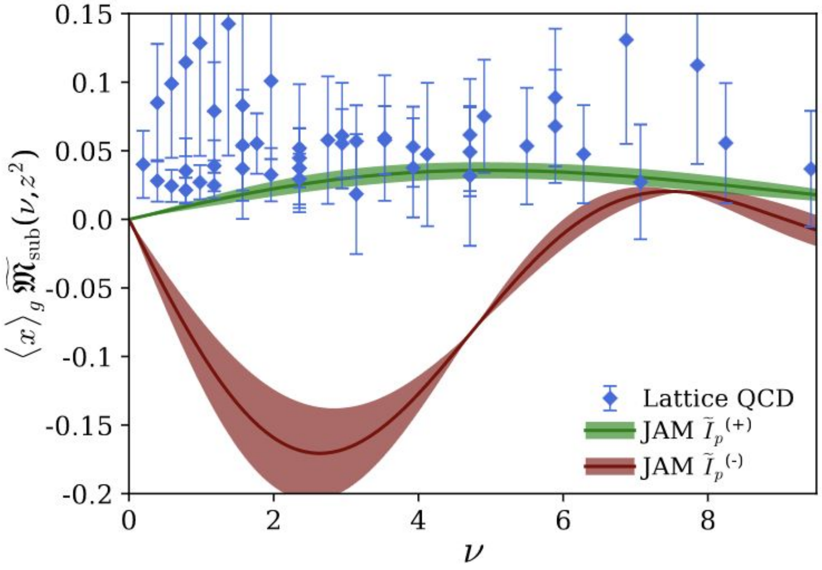

$$\widetilde{\mathfrak{M}}(\nu,z^2)\langle x_g\rangle_{\mu^2} = \widetilde{\mathcal{I}}_p(\nu,\mu^2) - \frac{\alpha_s N_c}{2\pi}\int_0^1 du\,\widetilde{\mathcal{I}}_p(u\nu,\mu^2)\Big\{\ln\Big(z^2\mu^2\frac{e^{2\gamma_E}}{4}\Big)\Big(\Big[\frac{2u^2}{\bar{u}}+4u\bar{u}\Big]_+ - \Big(\frac{1}{2}+\frac{4}{3}\frac{\langle x_S\rangle_{\mu^2}}{\langle x_g\rangle_{\mu^2}}\Big)\delta(\bar{u})\Big) + 4\Big[\frac{u+\ln(1-u)}{\bar{u}}\Big]_+ - \Big(\frac{1}{\bar{u}}-\bar{u}\Big)_+ - \frac{1}{2}\delta(\bar{u}) + 2\bar{u}u\Big\} - \frac{\alpha_s C_F}{2\pi}\int_0^1 du\,\widetilde{\mathcal{I}}_S(u\nu,\mu^2)\Big\{\ln\Big(z^2\mu^2\frac{e^{2\gamma_E}}{4}\Big)\mathcal{B}_{gq}(u) + 2\bar{u}u\Big\} + \mathcal{O}(\Lambda^2_{\rm QCD}z^2)\,,$$

$$\widetilde{\mathcal{I}}_p(\nu) = \frac{i}{2}\int_{-1}^{1} dx\, e^{-ix\nu}\, x\,\Delta g(x)\,.$$

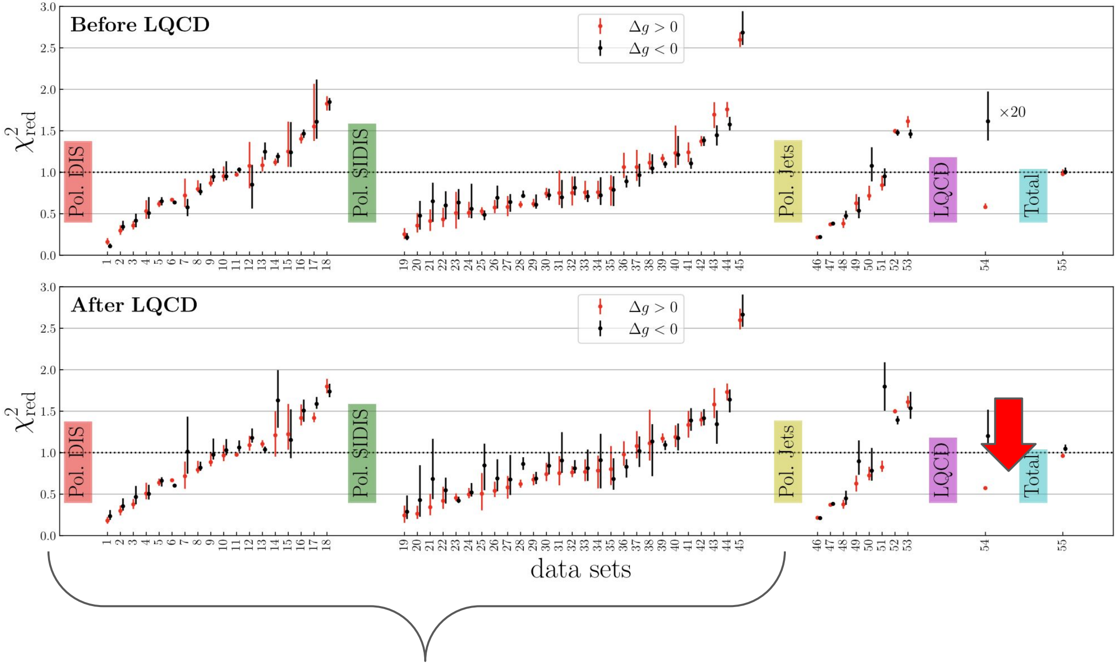

DIS W^2>10 GeV^2

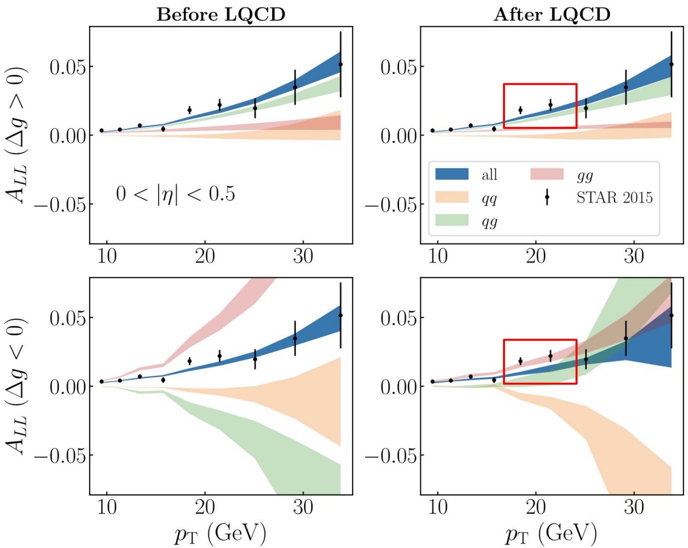

- Good description of global data after inclusion of LQCD for both solutions for g-hpdf

- On the basis of χ^2, LQCD cannot discriminate fully the sign of g-hpdf

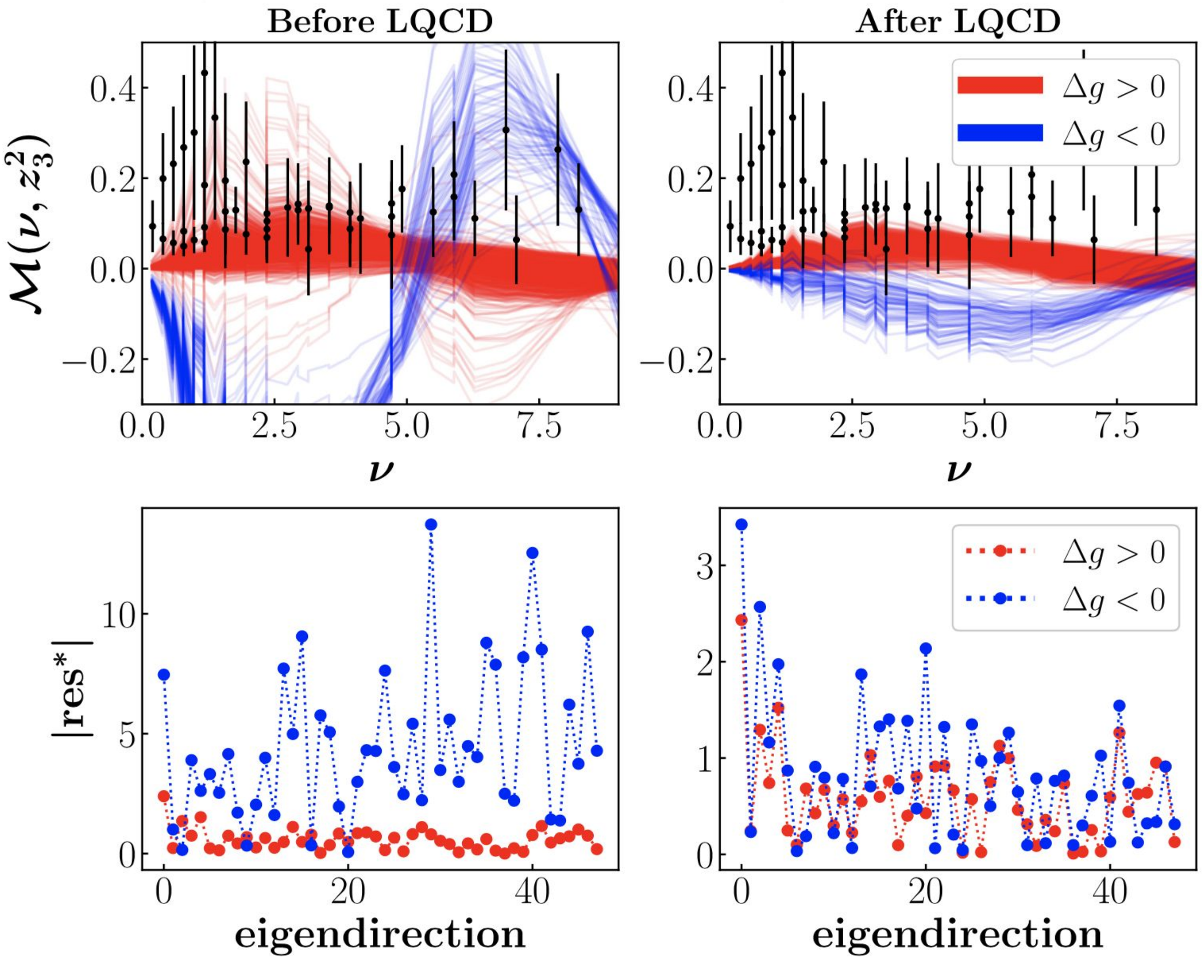

$$\chi^2 = (\boldsymbol{d}-\boldsymbol{t})^T \boldsymbol{\Sigma}^{-1} (\boldsymbol{d}-\boldsymbol{t})$$
$$= (\boldsymbol{d}-\boldsymbol{t})^T \boldsymbol{U} \boldsymbol{D}^{-1} \boldsymbol{U}^T (\boldsymbol{d}-\boldsymbol{t})$$
$$= \sum_i \mathrm{res}_i^{*2}.$$

- PCA projections of residuals reveal strong correlations between LQCD data points
- The correlations prevent determination of g-hpdf sign

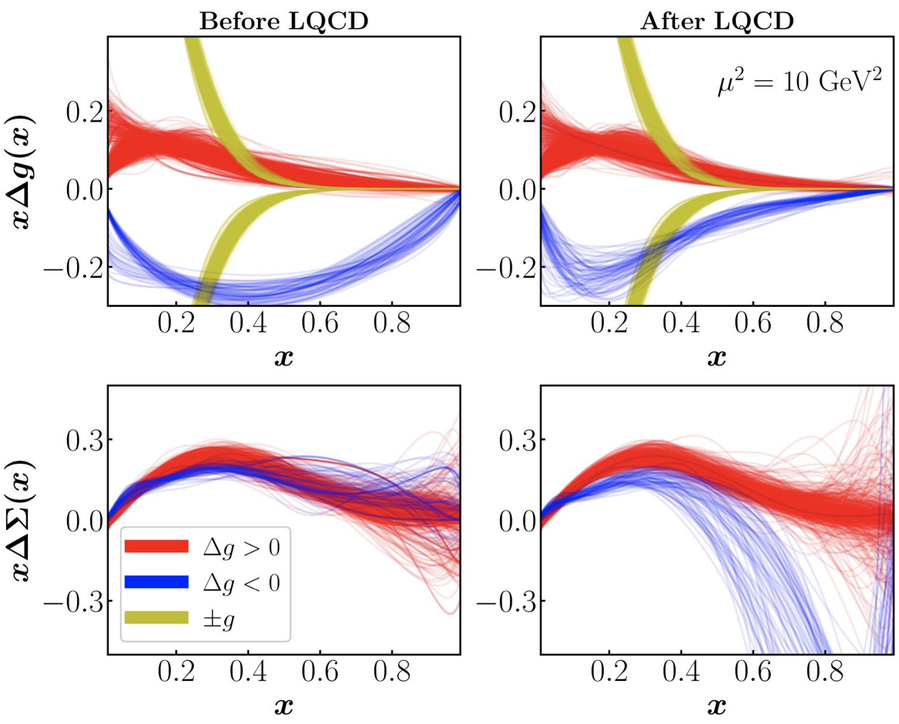

- LQCD distorts significantly the negative g-hpdf at higher x > 0.3
- Note that both solutions violate pdf positivity bounds for x > 0.3
- Before inclusion of LQCD data, singlet-hpdf were stable for both solutions
- Inclusion of LQCD data forces the quark singlet-hpdf to become negative at x > 0.4 for the negative g-hpdf

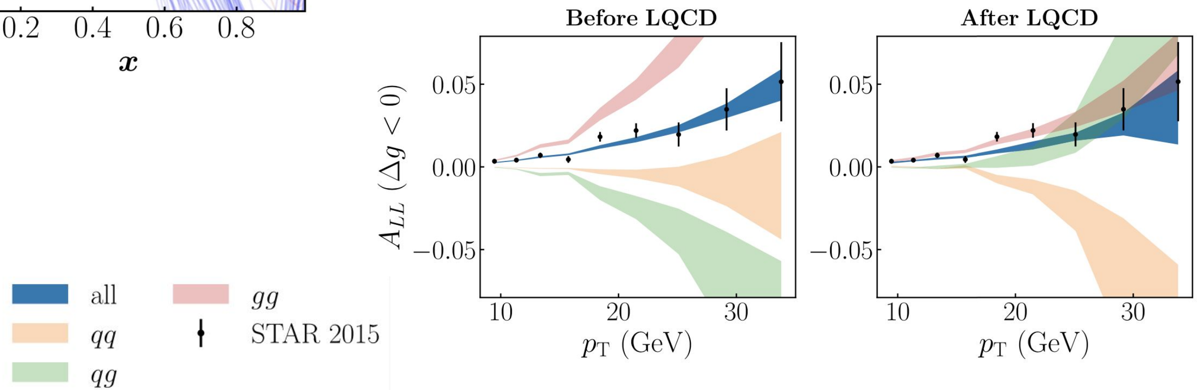

On the resolution of the sign of gluon polarization in the proton

N. T. Hunt-Smith,[1] C. Cocuzza,[2] W. Melnitchouk,[3] N. Sato,[3] A. W. Thomas,[1] and M. J. White[1]

[1] *CSSM and ARC Centre of Excellence for Dark Matter Particle Physics, Department of Physics, University of Adelaide, Adelaide 5005, Australia*

[2] *Department of Physics, William and Mary, Williamsburg, Virginia 23185, USA*

[3] *Jefferson Lab, Newport News, Virginia 23606, USA*

JAM Collaboration

(Dated: March 14, 2024)

Higgs production at RHIC and the positivity of the gluon helicity distribution

Daniel de Florian[a], Stefano Forte[b], Werner Vogelsang[c]

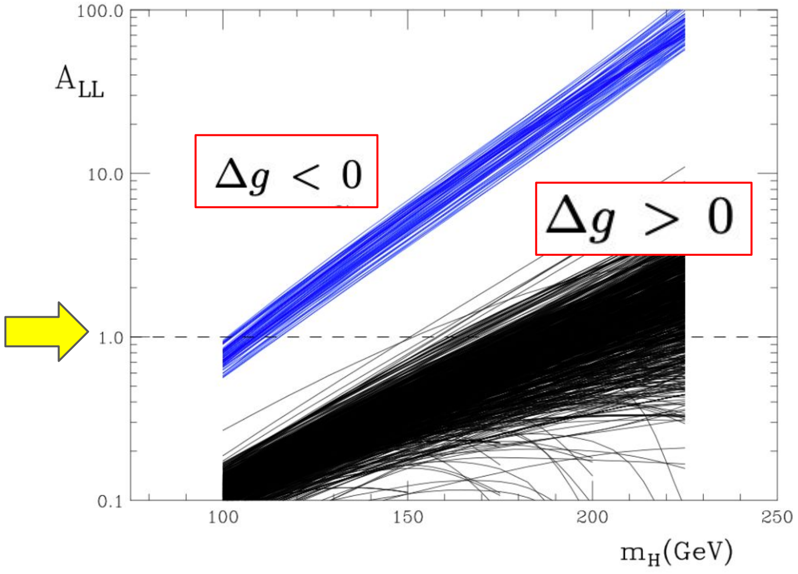

- Higgs A_LL is directly sensitive to g-hpdf squared at LO

- Calculations of A_LL(H) with negative g-hpdf can lead to unphysical results **(using non-LQCD based analysis)**

$$A_{LL}^{\mathrm{H}}(\tau) = \frac{[\Delta g \otimes \Delta g]}{[g \otimes g]} + \mathcal{O}(\alpha_s),$$

Can Higgs A_LL fully discriminate negative g-hpdf?

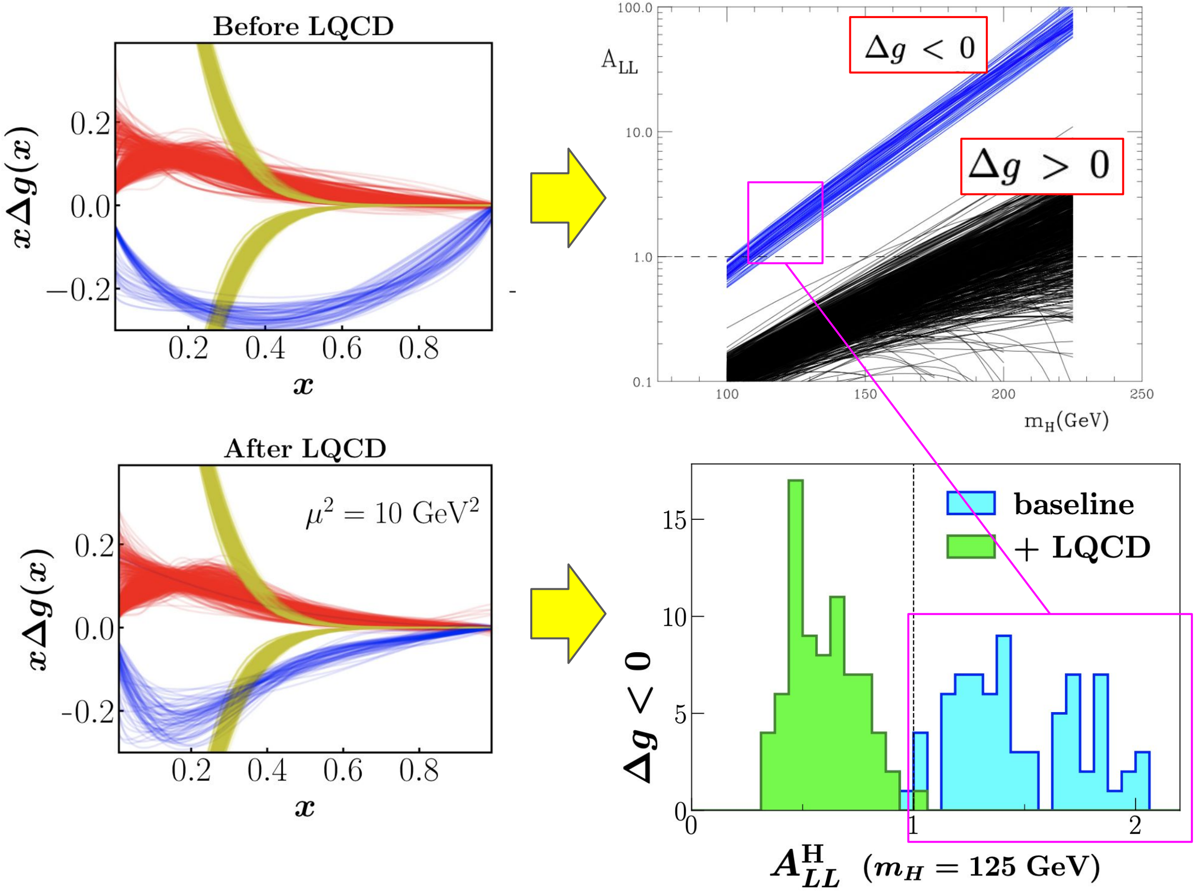

Negative g-hpdf with LQCD constraints still admits a physical Higgs A_LL

Reaction	$\chi^2_{\rm red}(\Delta g > 0)$ baseline	$\chi^2_{\rm red}(\Delta g > 0)$ + LQCD	$\chi^2_{\rm red}(\Delta g > 0)$ + high-x DIS	$\chi^2_{\rm red}(\Delta g < 0)$ baseline	$\chi^2_{\rm red}(\Delta g < 0)$ + LQCD	$\chi^2_{\rm red}(\Delta g < 0)$ + high-x DIS	N
Polarized							
Inclusive DIS	0.95	0.96	1.21	0.98	1.12	1.25	1735*
SIDIS	0.85	0.84	1.08	0.84	0.96	1.11	231
Inclusive jets	0.84	0.89	0.90	0.88	1.10	1.44	83
Inclusive $W^\pm/Z$	0.60	0.60	0.99	0.83	0.84	1.32	18
Total	**0.89**	**0.90**	**1.18**	**0.92**	**1.06**	**1.24**	**2067**
Unpolarized							
Inclusive DIS	1.17	1.17	1.17	1.18	1.18	1.19	3908
SIDIS	0.99	0.99	1.04	0.99	0.99	1.02	1490
Inclusive jets	1.28	1.28	1.30	1.29	1.29	1.30	198
Drell-Yan	1.21	1.21	1.21	1.24	1.24	1.24	205
Inclusive $W^\pm/Z$	1.01	1.01	1.01	1.03	1.03	1.04	153
Total	**1.14**	**1.14**	**1.14**	**1.15**	**1.15**	**1.15**	**5954**
SIA	0.86	0.86	0.89	0.90	0.90	0.92	564
LQCD	—	0.57	0.58	—	1.18	3.92	48
Total	**1.08**	**1.10**	**1.13**	**1.10**	**1.12**	**1.17**	**8633**

1370 additional data points for pol DIS (+ high-x DIS)

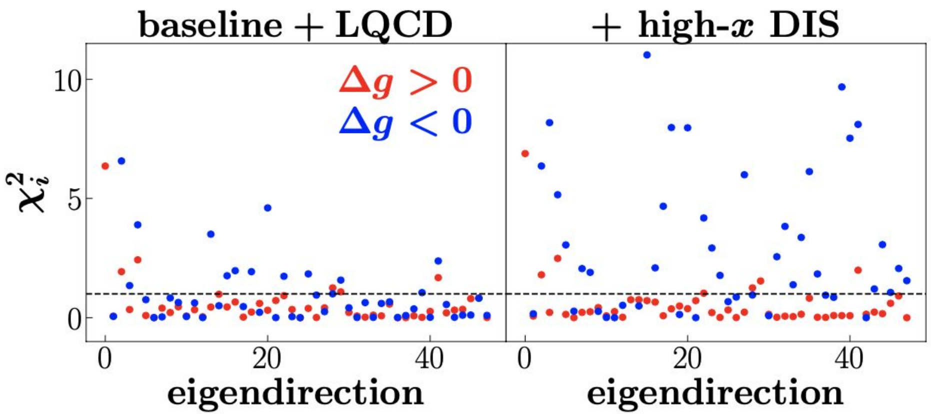

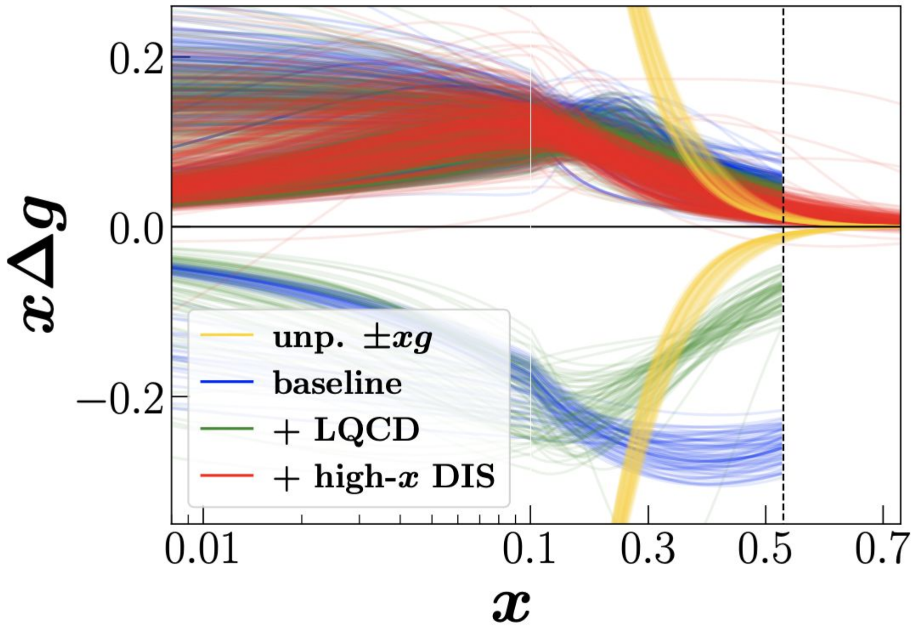

- With inclusion of high-x DIS DSAs, LQCD data strongly disfavor negative g-hpdf solution
- Combined DSA from jet and high-x DIS with LQCD allows us to discriminate the sign of g-hpdf for the first time!

Summary

- For the first time, we were able to discriminate the sign of g-hpdf using data-driven approach
- Constraints from LQCD along with DSAs from jets and DIS at large-x were crucial to achieve the resolution of g-hpdf sign
- Inclusion of LQCD is becoming increasingly important in global analysis
- Experimental constraints at large x on gluon - hpdf are still scarce, and more data needed to reach precision similar to unpolarized gluon density (EIC - small x, JLab12/22 - high x)

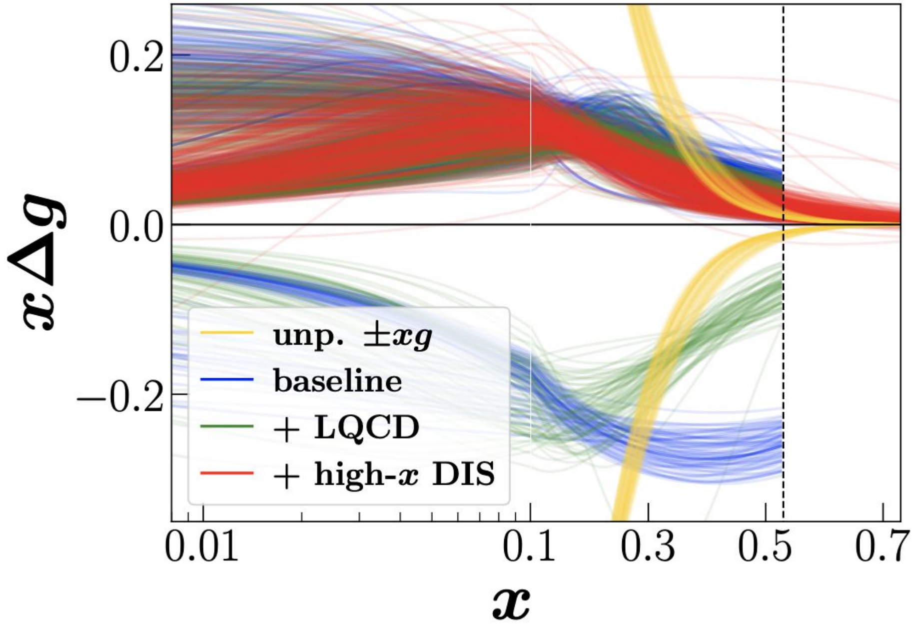

Transversity from Dihadron Transverse-Spin Observables

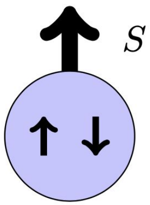

$$\delta_{\mathrm{T}} f = f_{\uparrow} - f_{\downarrow}$$

Transversity

Pitonyak, Cocuzza, Metz, Prokudin, NS, `24 (PRL)
Cocuzza, Metz, Pitonyak, Prokudin, NS, Seidl `24 (PRL)
Cocuzza, Metz, Pitonyak, Prokudin, NS, Seidl `24 (PRD)

Motivations

Gamberg, Malda, Miller, Pitonyak, Prokudin, NS, `22 (PRD)

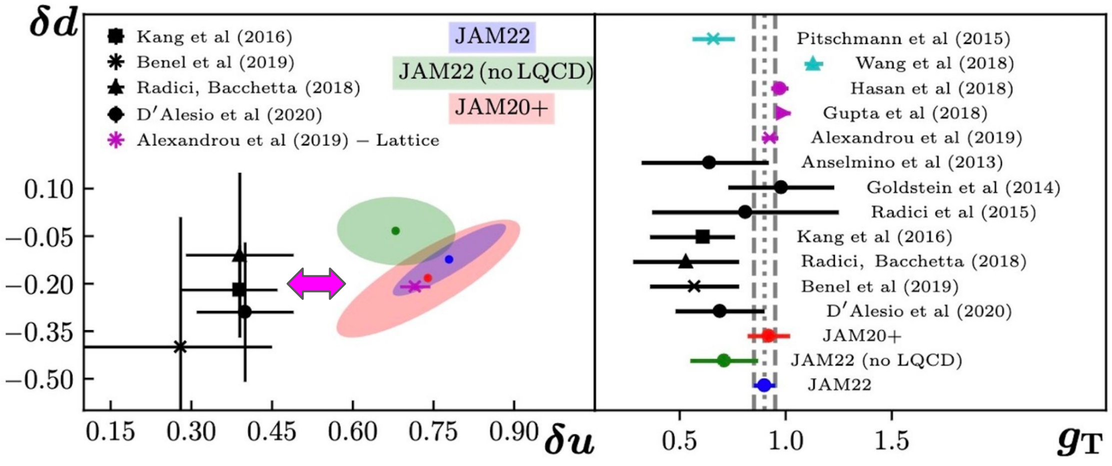

- TMD+CT3 pheno in tension with other analyzes (delta u)
- Radici, Bacchetta, and Benel, Courtoy, Ferro-Hernandez used collinear di-hadron observables to extract tensor charges
- New fresh look at collinear di-hadron pheno

Observable	Reactions	Non-Perturbative Function(s)	χ^2/npts	Exp. Refs.
$A_{UT}^{\sin(\phi_h-\phi_S)}$	$e+(p,d)^\uparrow \to e+(\pi^+,\pi^-,\pi^0)+X$	$f_{1T}^\perp(x,\vec{k}_T^2)$	$182.9/166 = 1.10$	[22, 24, 27]
$A_{UT}^{\sin(\phi_h+\phi_S)}$	$e+(p,d)^\uparrow \to e+(\pi^+,\pi^-,\pi^0)+X$	$h_1(x,\vec{k}_T^2), H_1^\perp(z,z^2\vec{p}_T^2)$	$181.0/166 = 1.09$	[22, 24, 27]
$^*A_{UT}^{\sin\phi_S}$	$e+p^\uparrow \to e+(\pi^+,\pi^-,\pi^0)+X$	$h_1(x), \tilde{H}(z)$	$18.6/36 = 0.52$	[22, 24, 27]
$A_{UC/UL}$	$e^+ + e^- \to \pi^+\pi^-(UC,UL)+X$	$H_1^\perp(z,z^2\vec{p}_T^2)$	$154.9/176 = 0.88$	[29–32]
$A_{T,\mu^+\mu^-}^{\sin\phi_S}$	$\pi^- + p^\uparrow \to \mu^+\mu^- + X$	$f_{1T}^\perp(x,\vec{k}_T^2)$	$6.92/12 = 0.58$	[34]
$A_N^{W/Z}$	$p^\uparrow + p \to (W^+,W^-,Z)+X$	$f_{1T}^\perp(x,\vec{k}_T^2)$	$30.8/17 = 1.81$	[35]
A_N^π	$p^\uparrow + p \to (\pi^+,\pi^-,\pi^0)+X$	$h_1(x), F_{FT}(x,x) = \frac{1}{\pi} f_{1T}^{\perp(1)}(x), H_1^{\perp(1)}(z), \tilde{H}(z)$	$70.4/60 = 1.17$	[7, 9, 10, 13]
Lattice g_T	——	$h_1(x)$	$1.82/1 = 1.82$	[89]

Analysis setup

Collaboration	References	Observable	Process	Nonperturbative function(s)
Belle	[64]	$d\sigma/dz\,dM_h$	$e^+e^- \to (\pi^+\pi^-)X$	D_1
Belle	[112]	$A^{e^+e^-}$	$e^+e^- \to (\pi^+\pi^-)(\pi^+\pi^-)X$	$D_1, H_1^{\sphericalangle}$
HERMES	[118]	A_{UT}^{SIDIS}	$ep^\uparrow \to e'(\pi^+\pi^-)X$	$D_1, H_1^{\sphericalangle}, h_1$
COMPASS	[117]	A_{UT}^{SIDIS}	$\mu\{p,D\}^\uparrow \to \mu'(\pi^+\pi^-)X$	$D_1, H_1^{\sphericalangle}, h_1$
STAR	[97,121]	A_{UT}^{pp}	$p^\uparrow p \to (\pi^+\pi^-)X$	$D_1, H_1^{\sphericalangle}, h_1$
ETMC	[77]	$\delta u,\ \delta d$	LQCD	h_1
PNDME	[71]	$\delta u,\ \delta d$	LQCD	h_1

$$\frac{d\sigma}{dz\,dM_h} = \frac{4\pi N_c \alpha_{\text{em}}^2}{3s}\sum_q \bar{e}_q^2 D_1^q(z, M_h),$$

$$A^{e^+e^-}(z, M_h, \bar{z}, \bar{M}_h) = \frac{\sin^2\theta \sum_q e_q^2 H_1^{\sphericalangle,q}(z, M_h) H_1^{\sphericalangle,\bar{q}}(\bar{z}, \bar{M}_h)}{(1+\cos^2\theta)\sum_q e_q^2 D_1^q(z, M_h) D_1^{\bar{q}}(\bar{z}, \bar{M}_h)}$$

$$A_{UT}^{\text{SIDIS}} = c(y)\frac{\sum_q e_q^2 h_1^q(x) H_1^{\sphericalangle,q}(z, M_h)}{\sum_q e_q^2 f_1^q(x) D_1^q(z, M_h)}$$

$$A_{UT}^{pp} = \frac{2P_{hT}\sum_i \sum_{a,b,c,d}\int_{x_a^{\min}}^1 dx_a \int_{x_b^{\min}}^1 \frac{dx_b}{z} h_1^a(x_a) f_1^b(x_b) \frac{d\Delta\hat{\sigma}_{a^\uparrow b \to c^\uparrow d}}{d\hat{t}} H_1^{\sphericalangle,c}(z, M_h)}{2P_{hT}\sum_i \sum_{a,b,c,d}\int_{x_a^{\min}}^1 dx_a \int_{x_b^{\min}}^1 \frac{dx_b}{z} f_1^a(x_a) f_1^b(x_b) \frac{d\hat{\sigma}_{ab \to cd}}{d\hat{t}} D_1^c(z, M_h)}$$

$h_1(x;\mu^2)$ Transversity (TPDF)

$H_1^{\sphericalangle}(z, M_h;\mu^2)$ Interference FF (IFF)

$D_1(z, M_h;\mu^2)$ Dihadron FF (DiFFs)

$$h_1(x;\mu^2)$$

$$H_1^{\sphericalangle}(z, M_h;\mu^2)$$

$$D_1(z, M_h;\mu^2)$$

Need to address scale dependence

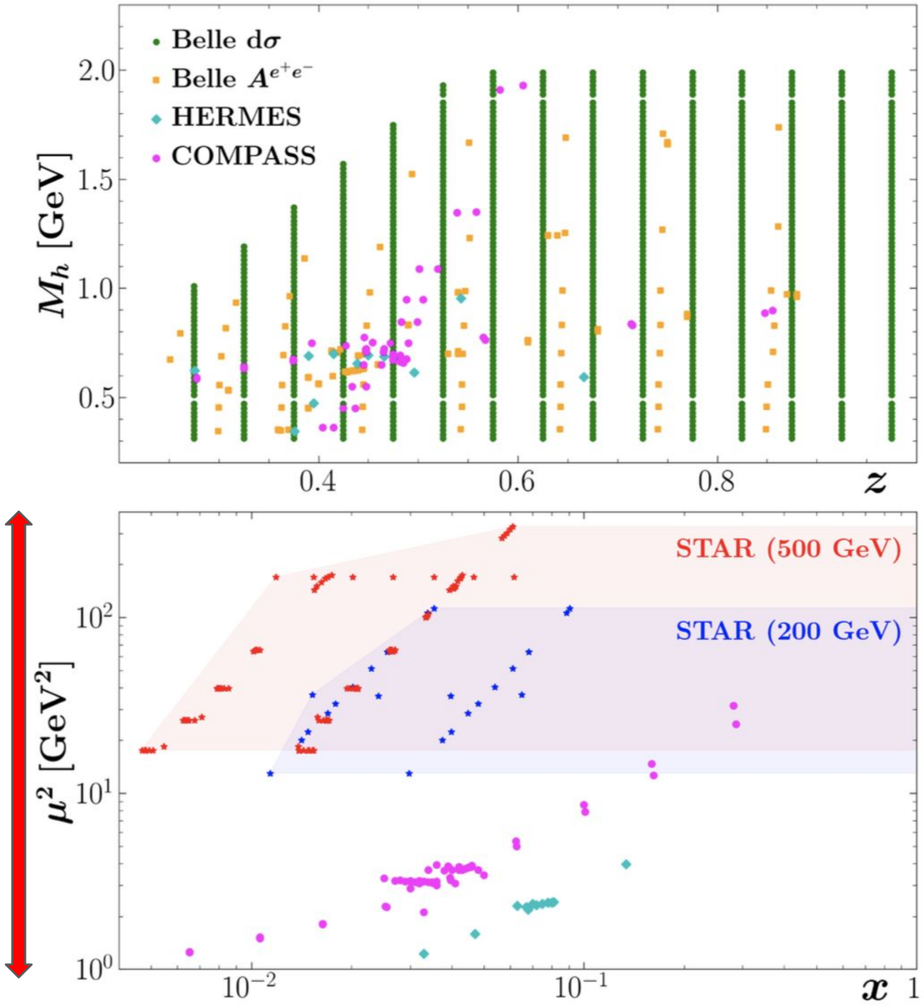

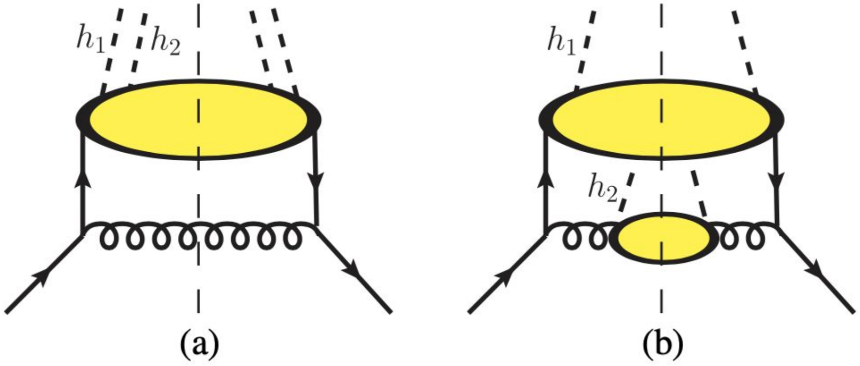

homogeneous inhomogeneous

- We work at LO in pQCD hence we only consider homogeneous evolution
- The scale dependence obeys standard timelike DGLAP evolution
- DGLAP only changes the z dependence

$$\frac{\partial D_1^{h_1 h_2/i}(z, M_h; \mu^2)}{\partial \mu^2} = \sum_j \int_z^1 \frac{dw}{w} D_1^{h_1 h_2/i}\left(\frac{z}{w}, M_h; \mu^2\right) P_{i \to j}(w)$$

Same for $H_1^{\sphericalangle}(z, M_h; \mu^2)$ with transversely polarized splitting kernels

Model assumptions in TPDF $h_1(x;\mu_0^2)$

- Traditional parametrization

$$h_1^i(x) = \frac{N^i}{\mathcal{M}^i} x^{\alpha^i}(1-x)^{\beta^i}(1+\gamma^i\sqrt{x}+\delta^i x)$$

- Reconstructed flavors

$$h_1^{u_v} \quad h_1^{d_v} \quad h_1^{\bar{u}_v} \quad h_1^{\bar{d}_v}$$

- Flavor assumptions (due to lack of observables)

$$h_1^{\bar{u}} = -h_1^{\bar{d}}$$

Expectations from large Nc limit

- Impose Soffer bounds

$$|h_1^i(x;\mu)| \leq \frac{1}{2}[f_1^i(x;\mu) + g_1^i(x;\mu)]$$

- Impose small-x constraints (Kovchegov, Sievert `19)

$$\alpha^i \xrightarrow{x\to 0} 1 - 2\sqrt{\frac{\alpha_s N_c}{2\pi}}. = 0.170 \pm 0.085$$

Added 50% conservative uncertainties

Model assumptions in DiFFs

$$D_1^{\pi^+\pi^-/i}(z, M_h; \mu_0^2)$$

- Mh grid based parametrization

$$D_1^i(z, \mathrm{M}_h^{i,j}) = \sum_{k=1,2,3} \frac{N_{jk}^i}{\mathcal{M}_{jk}^i} z^{\alpha_{jk}^i}(1-z)^{\beta_{jk}^i}$$

- Reconstructed flavors

$$D_1^u \quad D_1^s \quad D_1^c \quad D_1^b \quad D_1^g$$

- Flavor assumptions

$$D_1^u = D_1^d = D_1^{\bar{u}} = D_1^{\bar{d}},$$
$$D_1^s = D_1^{\bar{s}}, \qquad D_1^c = D_1^{\bar{c}}, \qquad D_1^b = D_1^{\bar{b}},$$

- Flavor separation using Pythia 6&8

$$\frac{\sigma^{q=s,c,b}}{\sigma^{\mathrm{tot}}} \Rightarrow$$

Generate Pythia data and assign uncertainties from various tunes

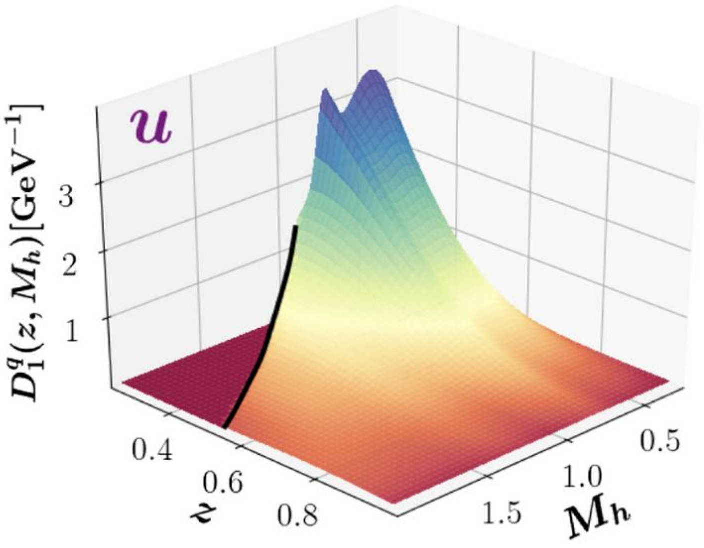

- Impose positivity

$$D_1^i(z, M_h; \mu) > 0,$$

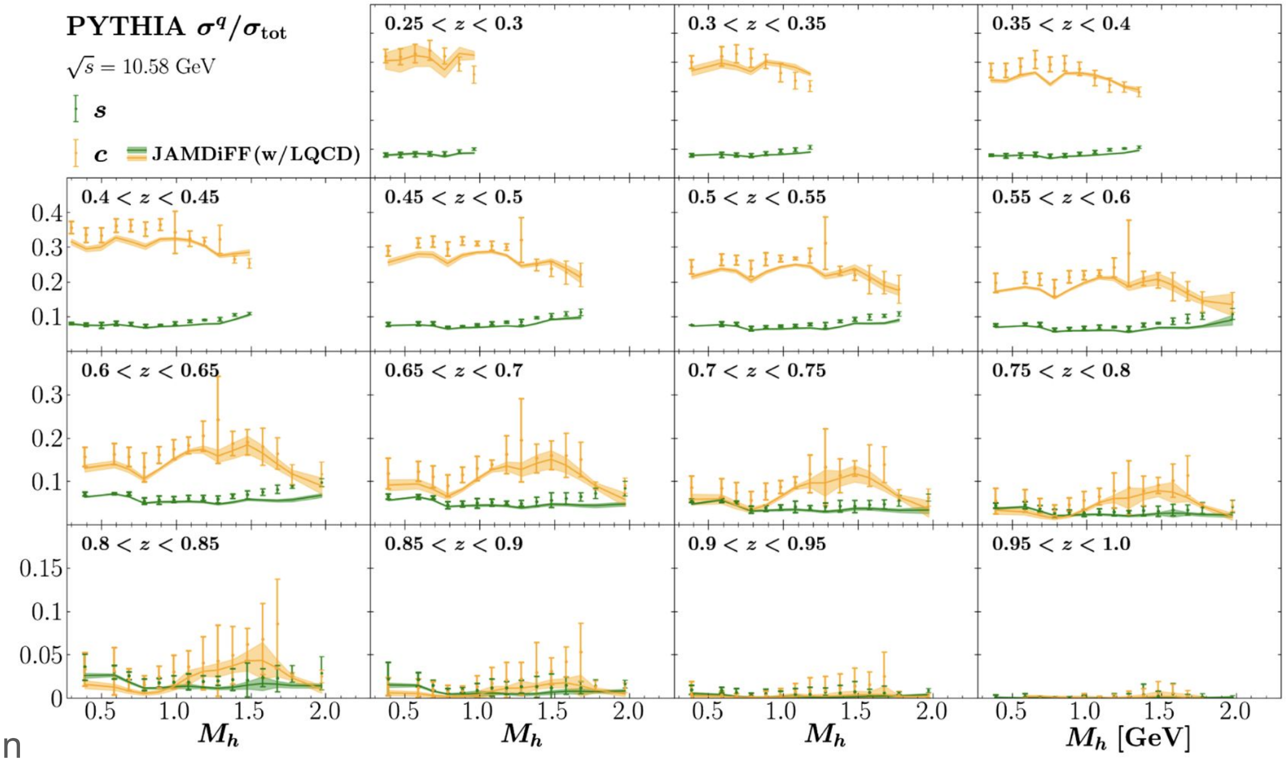

- Error bars on Pythia stemming from different tunes.

- Simulated Pythia data at different energies to constrain the gluon DiFF Q=10.58 - 91.19 GeV

Model assumptions in IFFs

$$H_1^{\sphericalangle,\pi^+\pi^-/i}(z, M_h; \mu_0^2)$$

- Mh grid based parametrization

$$H_1^{\sphericalangle,u}(z, \mathrm{M}_h^{u,j}) = \sum_{k=1,2} \frac{N_{jk}^u}{\mathcal{M}_{jk}^u} z^{\alpha_{jk}^u}(1-z)^{\beta_{jk}^u}$$

- Reconstructed flavors

$$H_1^{\sphericalangle,u}$$

- Flavor assumptions

$$H_1^{\sphericalangle,u} = -H_1^{\sphericalangle,d} = -H_1^{\sphericalangle,\bar{u}} = H_1^{\sphericalangle,\bar{d}},$$
$$H_1^{\sphericalangle,s} = H_1^{\sphericalangle,\bar{s}} = H_1^{\sphericalangle,c} = H_1^{\sphericalangle,\bar{c}} = H_1^{\sphericalangle,b} = H_1^{\sphericalangle,\bar{b}} = 0.$$

- Impose positivity bounds

$$|H_1^{\sphericalangle,i}(z, M_h; \mu)| < D_1^i(z, M_h; \mu)$$

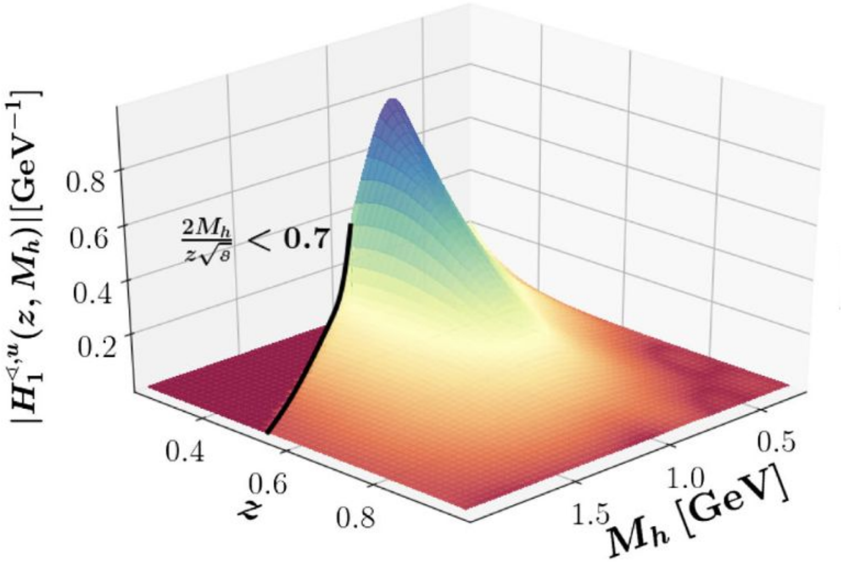

The results

Experiment	Binning	N_{dat}	χ^2_{red} JAMDiFF **(w/ LQCD)**	χ^2_{red} JAMDiFF **(no LQCD)**	χ^2_{red} JAMDiFF (SIDIS only)
Belle (cross section) [64]	z, M_h	1094	1.01	1.01	1.01
Belle (Artru-Collins) [112]	z, M_h	55	1.27	1.24	1.28
	$M_h, \overline{M}_h$	64	0.60	0.60	0.60
	$z, \bar{z}$	64	0.42	0.42	0.41
HERMES [118]	x_{bj}	4	1.77	1.70	1.67
	M_h	4	0.41	0.42	0.47
	z	4	1.20	1.17	1.13
COMPASS (p) [117]	x_{bj}	9	1.98	0.65	0.59
	M_h	10	0.92	0.94	0.93
	z	7	0.77	0.60	0.63
COMPASS (D) [117]	x_{bj}	9	1.37	1.42	1.22
	M_h	10	0.45	0.37	0.38
	z	7	0.50	0.46	0.46
STAR [121] $\sqrt{s} = 200$ GeV $R < 0.3$	$M_h, \eta < 0$	5	2.57	2.56	
	$M_h, \eta > 0$	5	1.34	1.55	
	$P_{hT}, \eta < 0$	5	0.98	1.00	
	$P_{hT}, \eta > 0$	5	1.73	1.74	
	η	4	0.52	1.46	
STAR [97] $\sqrt{s} = 500$ GeV $R < 0.7$	$M_h, \eta < 0$	32	1.30	1.10	
	$M_h, \eta > 0$	32	0.81	0.78	
	$P_{hT}, \eta > 0$	35	1.09	1.07	
	η	7	2.97	1.83	
ETMC δu [77]		1	0.71		
ETMC δd [77]		1	1.02		
PNDME δu [71]		1	8.68		
PNDME δd [71]		1	0.04		
Total χ^2_{red} (N_{dat})			**1.01** (1475)	**0.98** (1471)	0.96 (1341)

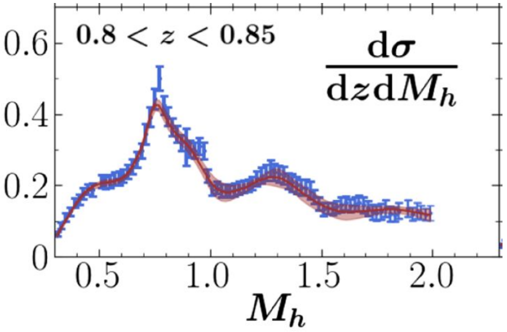

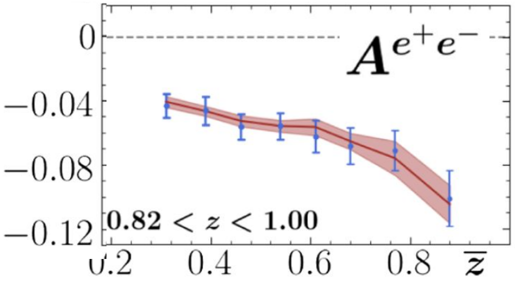

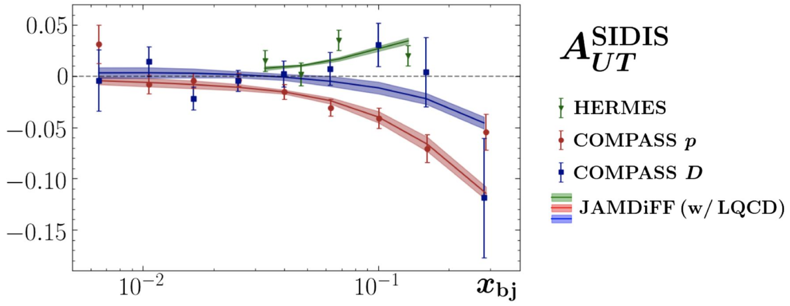

Reconstructed DiFFs

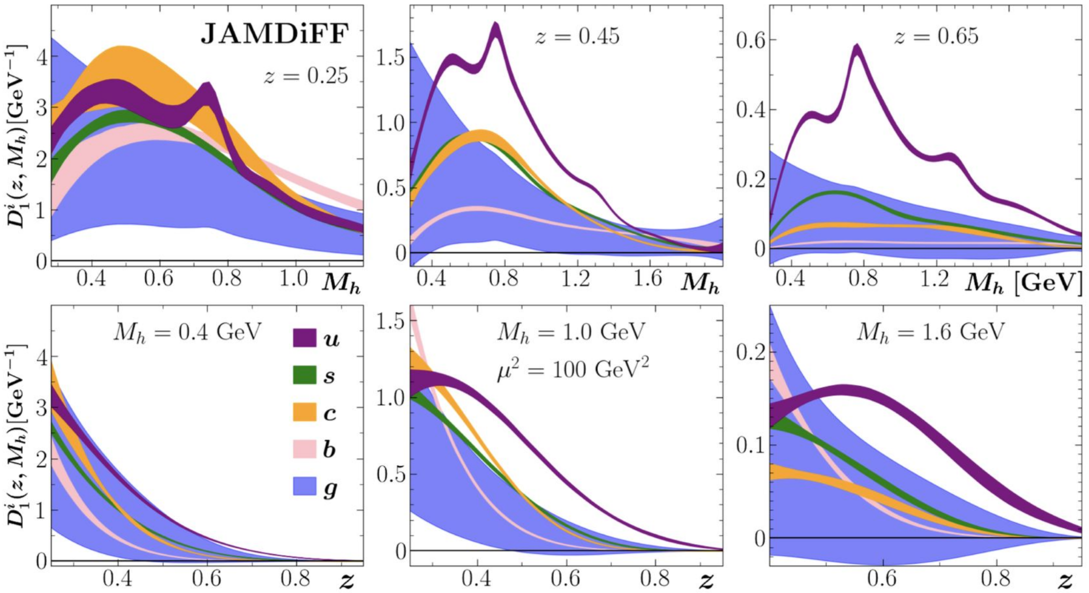

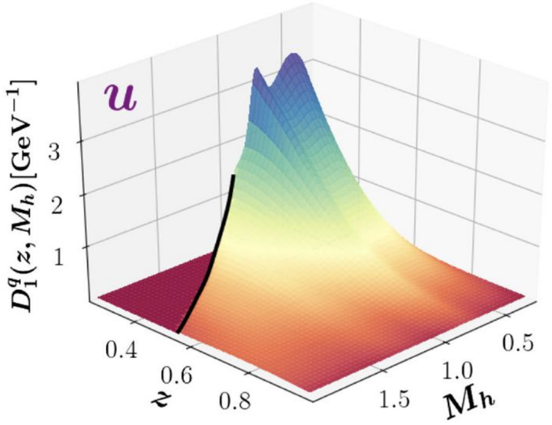

- More di-hadron pairs are produced at small z
- Clear reconstruction of the resonances
- DiFFs trend towards zero as we approach the physical threshold of 2mpi
- DiFFs goes to zero at large Mh as wide angle radiation is suppressed
- The gluon DiFF is not fully consistent with zero and more realistic than what was done in the past.

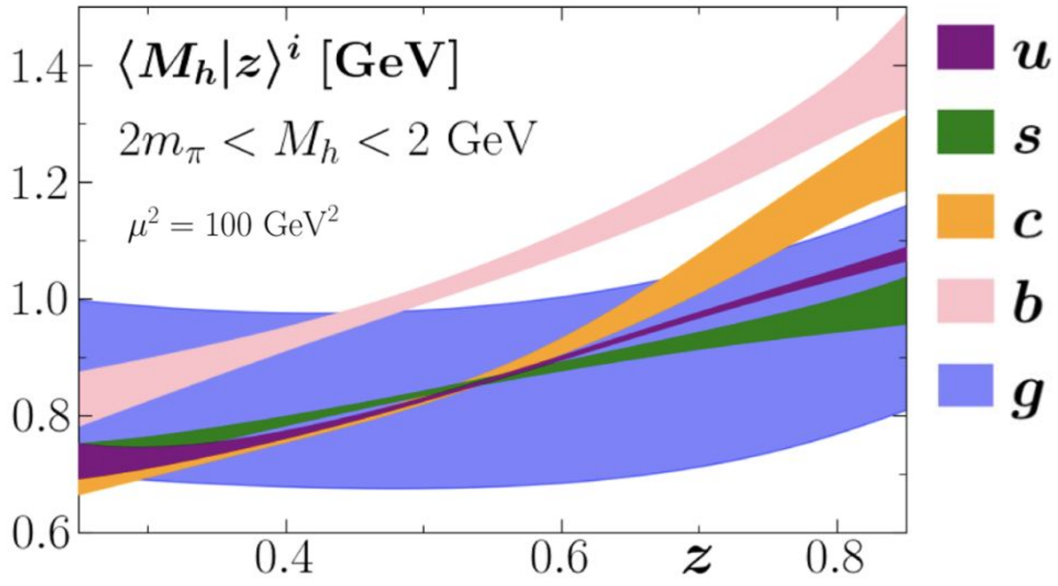

$$\langle M_h|z\rangle^i = \frac{\int \mathrm{d}M_h\, M_h\, D_1^i(z, M_h)}{\int \mathrm{d}M_h\, D_1^i(z, M_h)}$$

$$z = z_1 + z_2$$
$$M_h^2 = (P_{\pi^+} + P_{\pi^-})^2$$

- As expected, the invariant mass of the di-hadron pairs grows as z grows. Quark mass dependence becomes more important at large z
- At small z, large production of di-hadron pairs occurs, and quark masses does not influence the values of <Mh|z>
- Exception is the b-quark that due to its large mass generates larger Mh values

Reconstructed IFFs

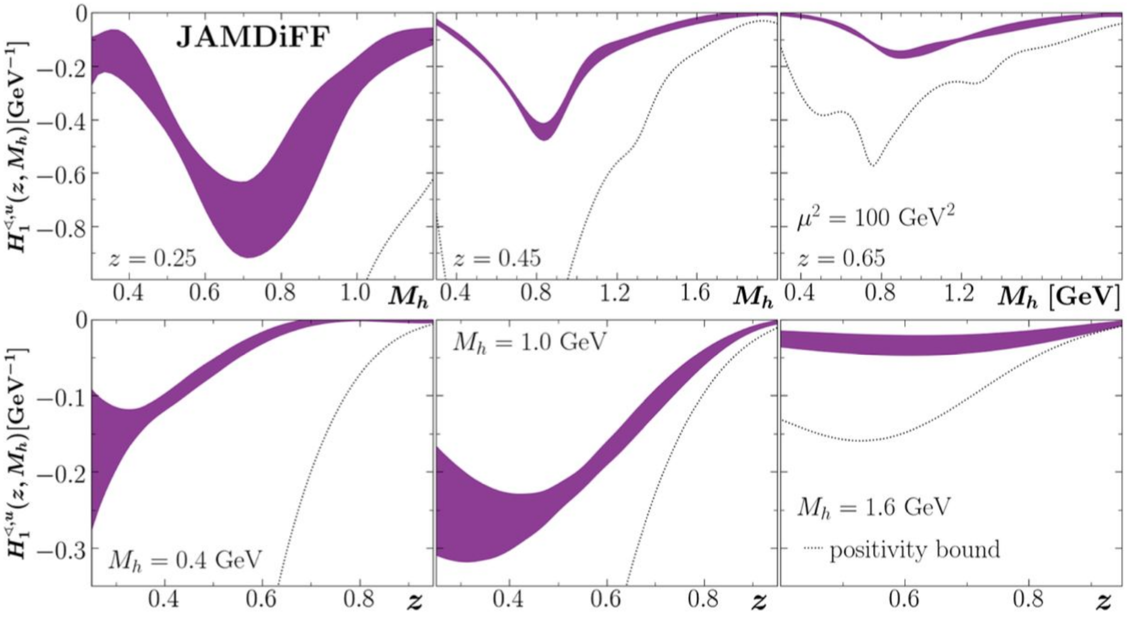

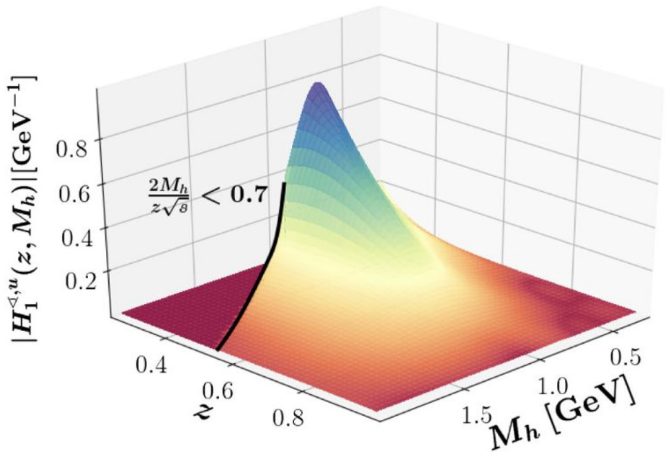

- Magnitude of IFF is proportional to DiFFs
- Marginal impact by positivity constraints
- The sign is not determined by the experimental data.

Reconstructed TPDF

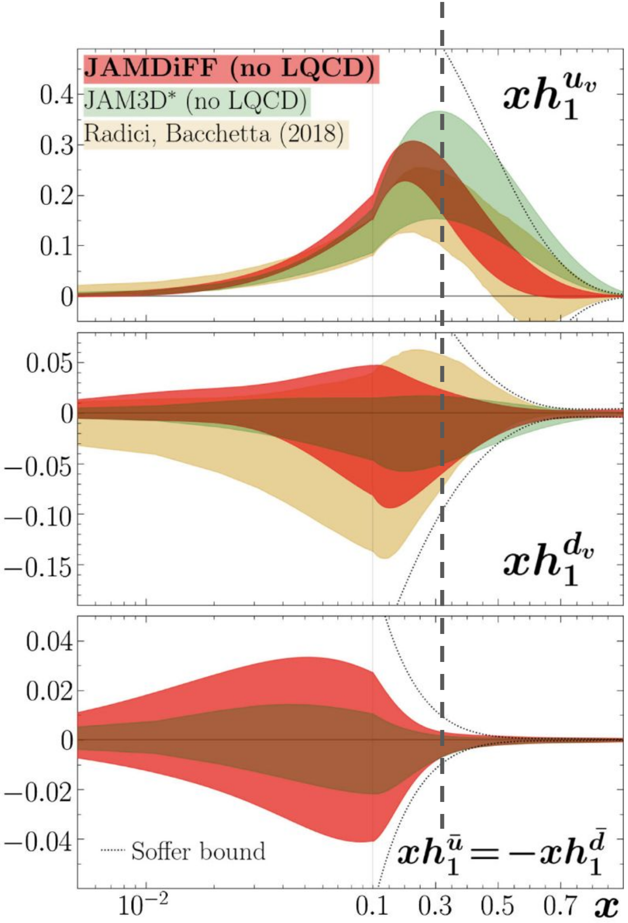

- Point-by-point in x constraints from data ends around x~0.3.
- Below x<0.3, the reconstructed transversity PDFs are consistent with Radici et al and TMD+CT3 (JAM3D) results.
- Beyond x>0.3, only the u quark PDF has non-vanishing signal with some differences wrt JAM3D*
- JAM3D* includes antiquarks and small x constraints

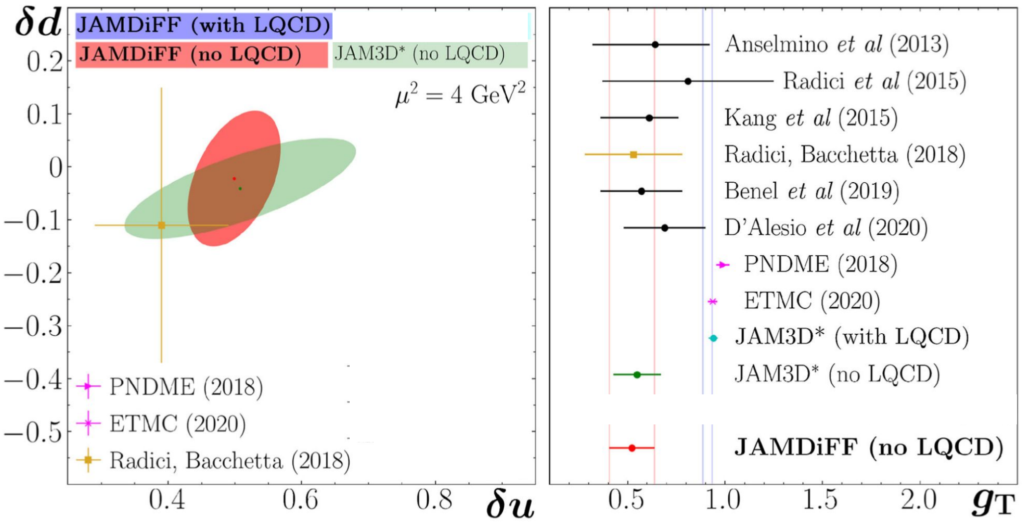

Reconstructed TPDF with LQCD

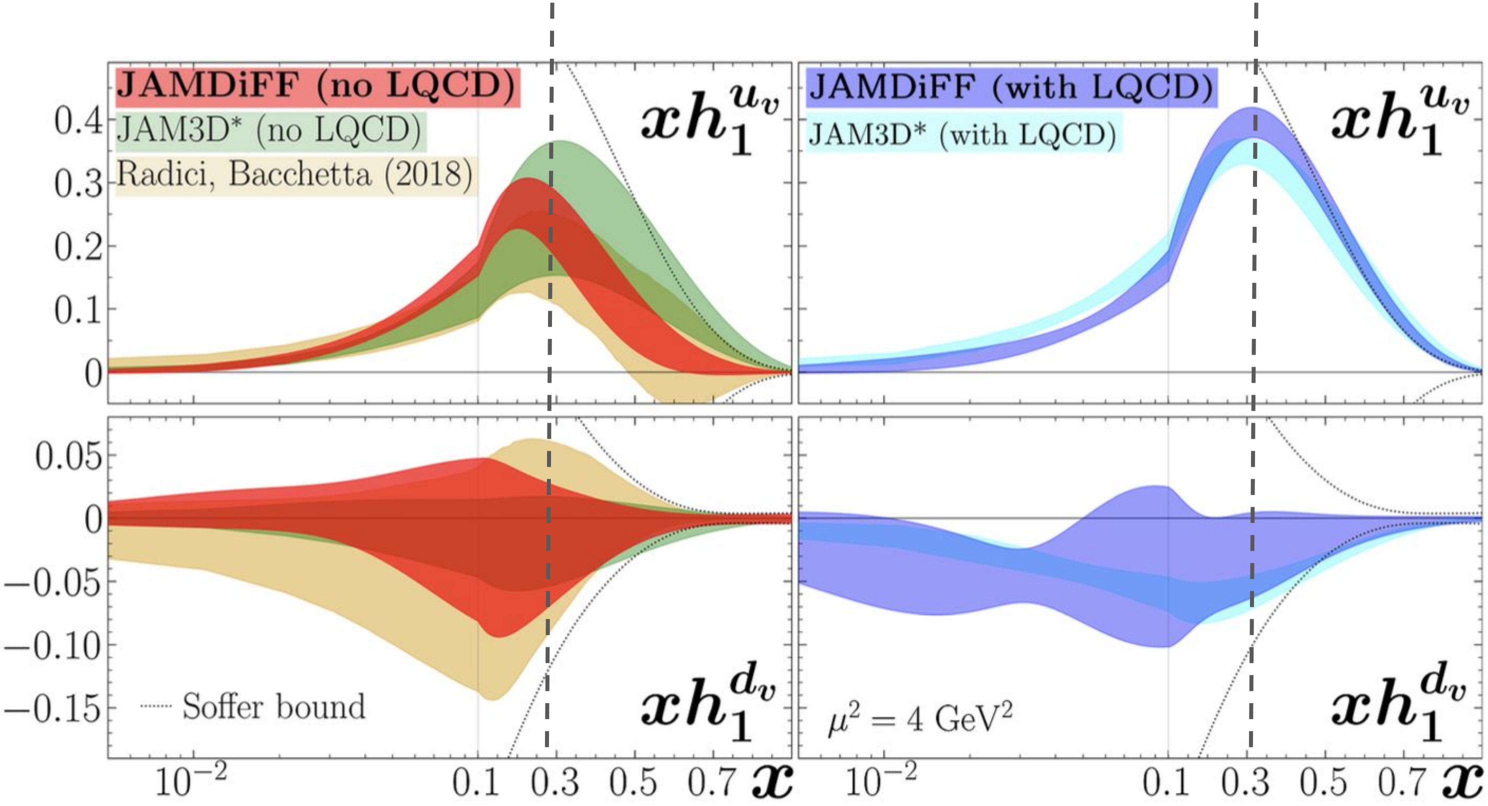

Reconstructed TPDF **with LQCD**

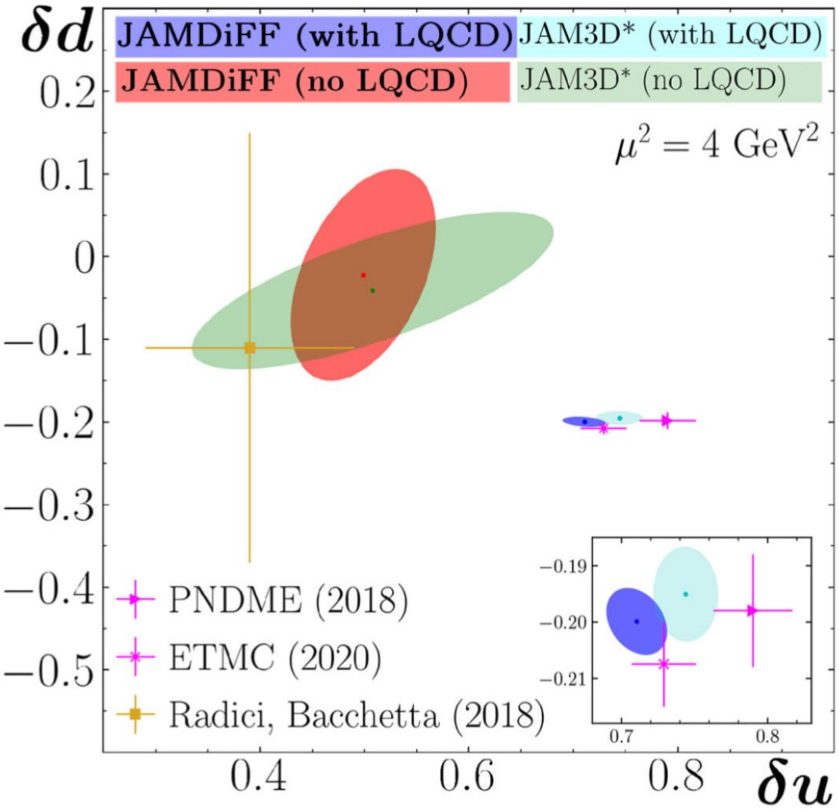

	χ^2_{red}	
	JAMDiFF	
Experiment	**(w/ LQCD)**	**(no LQCD)**
Belle (cross section) [64]	1.01	1.01
	1.27	1.24
Belle (Artru-Collins) [112]	0.60	0.60
	0.42	0.42
	1.77	1.70
HERMES [118]	0.41	0.42
	1.20	1.17
	1.98	0.65
COMPASS (p) [117]	0.92	0.94
	0.77	0.60
	1.37	1.42
COMPASS (D) [117]	0.45	0.37
	0.50	0.46
	2.57	2.56
STAR [121]	1.34	1.55
$\sqrt{s} = 200$ GeV	0.98	1.00
$R < 0.3$	1.73	1.74
	0.52	1.46
	1.30	1.10
STAR [97]	0.81	0.78
$\sqrt{s} = 500$ GeV	1.09	1.07
$R < 0.7$	2.97	1.83
ETMC δu [77]	0.71	
ETMC δd [77]	1.02	
PNDME δu [71]	8.68	
PNDME δd [71]	0.04	
Total χ^2_{red} (N_{dat})	**1.01** (1475)	**0.98** (1471)

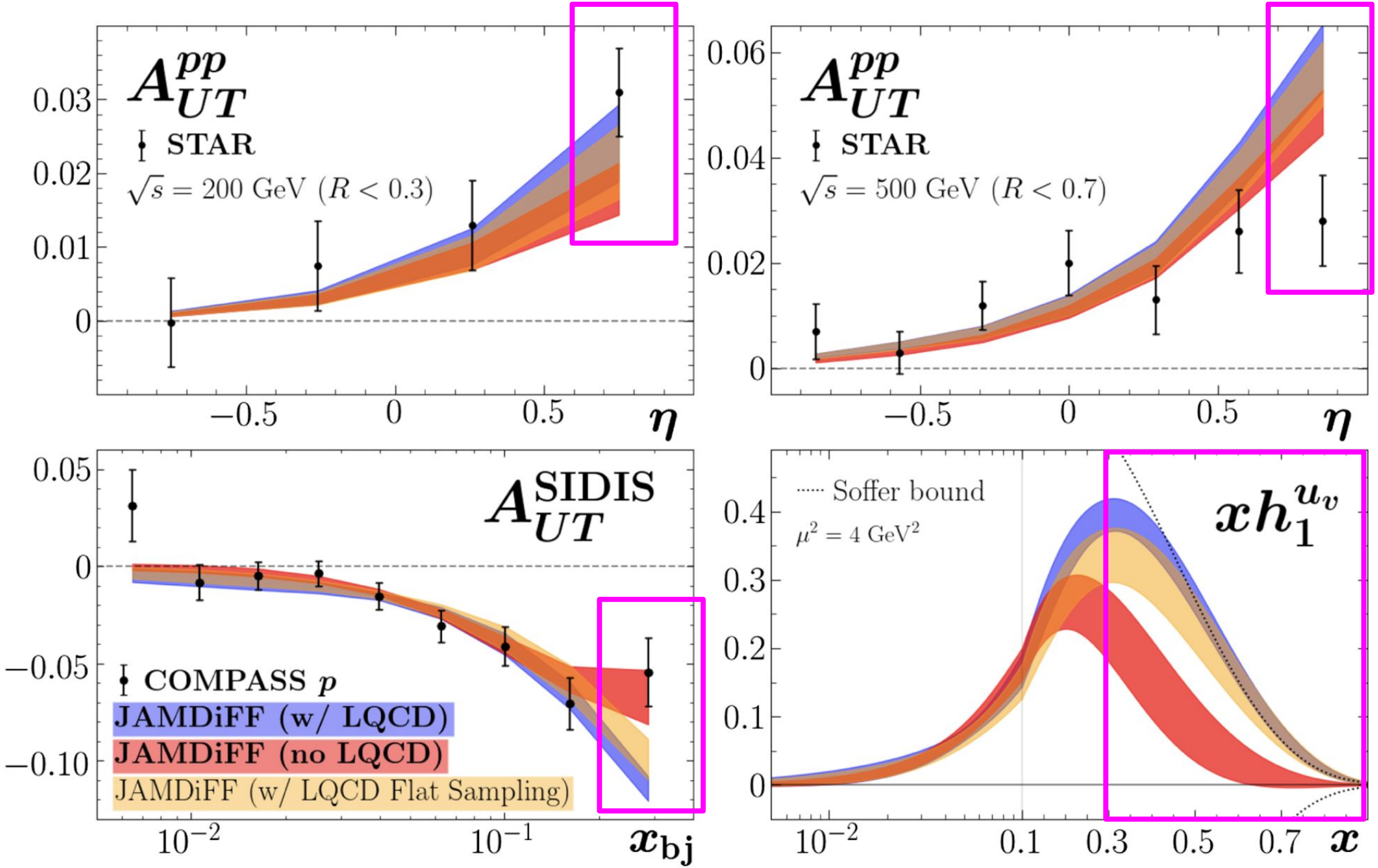

A_{UT}^{pp}
STAR
$\sqrt{s}$ = 200 GeV (R < 0.3)
η
A_{UT}^{pp}
STAR
$\sqrt{s}$ = 500 GeV (R < 0.7)
η
$A_{UT}^{\rm SIDIS}$
COMPASS p
JAMDiFF (w/ LQCD)
JAMDiFF (no LQCD)
JAMDiFF (w/ LQCD Flat Sampling)
$x_{\rm bj}$
Soffer bound
μ^2 = 4 GeV^2
$xh_1^{u_v}$
x

Summary

- At present there is no significant tension between LQCD and experimental reconstruction of nucleon tensor charges
- Different reconstructions of tensor charges are mostly driven by large x data
- More high x data is needed to reach accurate reconstruction of TPDF above x>0.3
- Inclusion of LQCD calculations as priors are very informative/useful in QCD phenomenology
- The JAMDiFF results and JAM3D* results are very similar and one can perform a combined analysis (TMD+CT3 & DiFF) **->** indicates possible **universal nature of all SSAs and nucleon tensor charges**